line at www.sciencemag.org/cgi/content/full/1069268/DC1.
14. C. Baugh, D. Grate, C. Wilson, *J. Mol. Biol.* **301**, 117 (2000).
15. W. A. Hendrickson, *Science* **254**, 51 (1991).
16. M. Costa, E. L. Christian, F. Michel, *RNA* **4**, 1055 (1998).
17. B. B. Konforti *et al.*, *Mol. Cell.* **1**, 433 (1998).
18. L. Zhang, J. Doudna, unpublished observations.
19. J. H. Cate *et al.*, *Science* **273**, 1678 (1996).
20. E. J. Sontheimer, P. M. Gordon, J. A. Piccirilli, *Genes Dev.* **13**, 1729 (1999).
21. A. M. Pyle, *Science* **261**, 709 (1993).
22. R. K. Sigel, A. Vaidya, A. M. Pyle, *Nature Struct. Biol.* **7**, 1111 (2000).
23. P. M. Gordon, J. A. Piccirilli, *Nature Struct. Biol.* **8**, 893 (2001).
24. R. K. Sigel, A. M. Pyle, personal communication.
25. J. H. Cate, R. L. Hanna, J. A. Doudna, *Nature Struct. Biol.* **4**, 553 (1997).
26. D. L. Abramovitz, R. A. Friedman, A. M. Pyle, *Science* **271**, 1410 (1996).
27. G. Chanfreau, A. Jacquier, *Science* **266**, 1383 (1994).
28. S. L. Yean, G. Wuenschell, J. Termini, R. J. Lin, *Nature* **408**, 881 (2000).
29. P. Z. Qin, A. M. Pyle, *Curr. Opin. Struct. Biol.* **8**, 301 (1998).
30. V. T. Chu, Q. Liu, M. Podar, P. S. Perlman, A. M. Pyle, *RNA* **4**, 1186 (1998).
31. V. T. Chu, C. Adamidi, Q. Liu, P. S. Perlman, A. M. Pyle, *EMBO J.* **20**, 6866 (2001).
32. J. A. Berglund, M. Rosbash, S. C. Schultz, *RNA* **7**, 682 (2001).
33. J. Wu, J. L. Manley, *Genes Dev.* **3**, 1553 (1989).
34. Y. Zhuang, A. M. Weiner, *Genes Dev.* **3**, 1545 (1989).
35. C. C. Query, M. J. Moore, P. A. Sharp, *Genes Dev.* **8**, 587 (1994).
36. R. Parker, P. G. Siliciano, C. Guthrie, *Cell* **49**, 229 (1987).
37. M. Carson, *J. Appl. Crystallogr.* **24**, 958 (1991).
38. D. L. Daniels, W. J. Michels, A. M. Pyle, *J. Mol. Biol.* **256**, 31 (1996).
39. A. R. Ferre-D'Amare, K. Zhou, J. A. Doudna, *Nature* **395**, 567 (1998).

40. The authors wish to thank A. Ferre-D'Amare for providing plasmid pD5627 and initiating the work, A. M. Pyle and R. Sigel for providing plasmid pJD13′-673 and sharing NMR data, the Yale Center for Structural Biology for crystallographic and computer support, J. Kieft, D. Battle, J. Murray, S. Szep, and the staff at the National Synchrotron Light Source for help with data collection. We also thank A. M. Pyle, J. Steitz, D. Rio, D. Battle, P. Adams, and B. Sagar for critical reading of this manuscript and insightful discussions, as well as C. Guthrie, R. Batey, and members of the Doudna laboratory for helpful discussions. This work was funded in part by a grant from the NIH. Coordinates of d56-TR have been deposited in the Protein Data Bank (RCSB ID code RCSB015439 and PDB ID code 1KXK).

21 December 2001; accepted 4 February 2002
Published online 21 February 2002;
10.1126/science.1069268
Include this information when citing this paper.

Living with Lethal PIP3 Levels: Viability of Flies Lacking PTEN Restored by a PH Domain Mutation in Akt/PKB

Hugo Stocker,[1] Mirjana Andjelkovic,[2]* Sean Oldham,[1] Muriel Laffargue,[3] Matthias P. Wymann,[3] Brian A. Hemmings,[2] Ernst Hafen[1]†

The phosphoinositide phosphatase PTEN is mutated in many human cancers. Although the role of PTEN has been studied extensively, the relative contributions of its numerous potential downstream effectors to deregulated growth and tumorigenesis remain uncertain. We provide genetic evidence in *Drosophila melanogaster* for the paramount importance of the protein kinase Akt [also called protein kinase B (PKB)] in mediating the effects of increased phosphatidylinositol 3,4,5-trisphosphate (PIP3) concentrations that are caused by the loss of PTEN function. A mutation in the pleckstrin homology (PH) domain of Akt that reduces its affinity for PIP3 sufficed to rescue the lethality of flies devoid of PTEN activity. Thus, Akt appears to be the only critical target activated by increased PIP3 concentrations in *Drosophila*.

Mutations in the tumor suppressor gene *PTEN* (the phosphatase and tensin homolog on chromosome 10) are frequent in glioblastomas, endometrial carcinoma, melanomas, and prostate cancer (*1*). Furthermore, two dominant hamartoma syndromes, Cowden disease and Bannayan-Zonana syndrome, are linked to germ line mutations in *PTEN* (*1*). The PTEN protein carries a phosphatase domain resembling those of dual-specificity protein phosphatases (*2–4*). Although it can dephosphorylate protein substrates such as focal adhesion kinase (*5*) and the adapter protein Shc (*6*), PTEN's predominant enzymatic activity appears to be the dephosphorylation of phosphoinositides at the D3 position. Because PTEN uses the second messenger PIP3 as a substrate, PTEN antagonizes the function of phosphatidylinositol-3 kinase (PI3K) (*7*, *8*). Immortalized mouse embryonic fibroblasts or embryonic stem cells lacking PTEN function show an approximately twofold increase in PIP3 concentrations (*9*, *10*). PIP3 interacts with a wide variety of PH domain-containing proteins, including the serine-threonine kinases Akt (also called PKB) and phosphoinositide-dependent kinase 1 (PDK1), Btk family tyrosine kinases, guanine nucleotide exchange factors for the Rho and Arf families of small guanosine triphosphatases, and phospholipase Cγ (*11*, *12*). The plethora of proteins that are potentially regulated by PIP3 provides widespread signaling potential for this lipid second messenger.

Genetic analyses in model organisms have implicated PTEN as a negative regulator of insulin receptor signaling. In the nematode *Caenorhabditis elegans*, PTEN antagonizes the activity of the PI3K AGE-1 in the regulation of metabolism, development, and life span (*13–16*). In the fruit fly *Drosophila melanogaster*, PTEN counteracts signaling downstream of the insulin receptor to control cellular growth (*17–19*). There are, however,

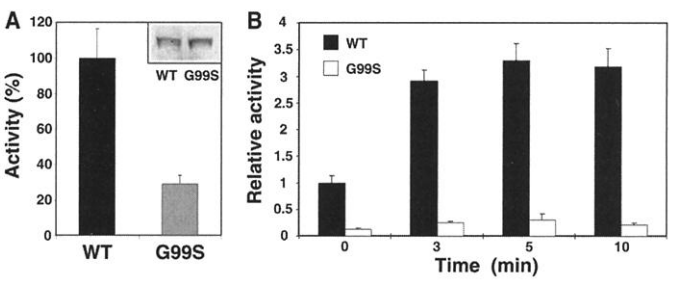

Fig. 1. Reduced kinase activity caused by an amino acid substitution in the PH domain of dAkt. (**A**) Effect of the G99S substitution in the PH domain on dAkt kinase activity from larval extracts (*42*). Activity from wild-type larvae was considered to be 100%. Inset, dAkt protein was detected in 40 μg of larval extracts using the same antiserum. (**B**) Reduced insulin-induced activation of the G99S mutant dAkt. The dAkt constructs were expressed in HEK 293 cells (*43*). Transfected cells were starved for 24 hours before stimulation with insulin for the indicated time periods, and dAkt kinase activity was determined (*44*). The activity of wild-type dAkt from unstimulated cells was considered to be relative activity = 1.

[1]Zoologisches Institut der Universität Zürich, Winterthurerstrasse 190, CH-8057 Zürich, Switzerland. [2]Friedrich Miescher Institute, Maulbeerstrasse 66, CH-4058 Basel, Switzerland. [3]Université de Fribourg, Rue du Musée 5, CH-1700 Fribourg, Switzerland.

*Present address: Department of Vascular and Metabolic Diseases, F. Hoffmann-La Roche AG, CH-4070 Basel, Switzerland.

†To whom correspondence should be addressed. E-mail: hafen@zool.unizh.ch

additional phenotypes associated with mutations in *PTEN* that cannot easily be reconciled with an exclusive function of PTEN in insulin receptor signaling [for example, the burst vulva phenotype in *C. elegans* (*13*) and defects in the actin cytoskeleton in *Drosophila* (*17*)]. To better understand the consequences of loss of PTEN function, it would be useful to know which important downstream effectors react to increased PIP3 concentrations and whether PTEN has other physiological substrates in addition to PIP3.

The protein kinase Akt is an important component of insulin receptor signaling (*20*). Akt is recruited to the plasma membrane by virtue of the interaction of its NH_2–terminally located PH domain with PIP3. At the membrane, subsequent phosphorylation events by PDK1 and an unidentified kinase lead to the full activation of Akt (*21–23*). In *PTEN*-deficient mouse embryonic fibroblasts and embryonic stem cells, Akt is phosphorylated and activated (*9*, *10*). The phenotypes associated with *Akt* mutations in both *C. elegans* and *Drosophila* are consistent with its role in signal transduction downstream of the insulin receptor (*24–27*).

We monitored three properties of *Drosophila* Akt (dAkt) separately: kinase activity, abundance of the protein, and membrane localization. We relied entirely on mutations in the endogenous gene encoding dAkt to avoid potential side effects caused by overexpression of mutant proteins. $dAkt^{1}$ encodes a catalytically inactive protein, dAktF327I (*25*). The viable $dAkt^{4226}$ allele contains a P-element insertion upstream of the *dAkt* gene and therefore results in the reduced expression of wild-type dAkt protein (*19*, *28*). Finally, we characterized the viable hypomorphic mutation $dAkt^{3}$ (*29*) that selectively impairs the membrane recruitment of dAkt in response to increased concentrations of PIP3. Sequencing of genomic DNA extracted from $dAkt^{3}$ homozygous flies revealed a single nucleotide exchange resulting in the substitution of a serine residue for a nonconserved glycine at the end of the sixth β sheet of the PH domain. To address the mechanism by which this $Gly^{99} \rightarrow Ser^{99}$ (G99S) mutation in the PH domain affects dAkt, we compared the amount of dAkt protein and activity in wild-type and $dAkt^{3}$ mutant larvae. Whereas no apparent difference in expression of the protein was observed (Fig. 1A, inset), dAkt activity from the mutant larvae represented only 30% of that in wild-type larval extracts (Fig. 1A). We also expressed epitope-tagged forms of wild-type dAkt, catalytically inactive dAktF327I, and PH domain mutant dAktG99S in insulin-responsive human embryonic kidney (HEK) 293 cells. All three proteins were expressed in similar amounts (*30*). dAktG99S activity from insulin-stimulated cells was reduced by about 90% as compared to that of the wild-type kinase (Fig. 1B). All forms of dAkt proteins were detected in the cytosol of unstimulated cells (Fig. 2, A, D, and G). Stimulation of the cells with insulin for 5 min resulted in association of the wild-type and the catalytically inactive enzymes with the plasma membrane, but failed to recruit the dAktG99S mutant protein (Fig. 2, B, E, and H). In contrast, treatment of HEK 293 cells with the protein-tyrosine phosphatase inhibitor pervanadate, a potent activator of Akt (*31*), led to membrane recruitment of all dAkt proteins (Fig. 2, C, F, and J).

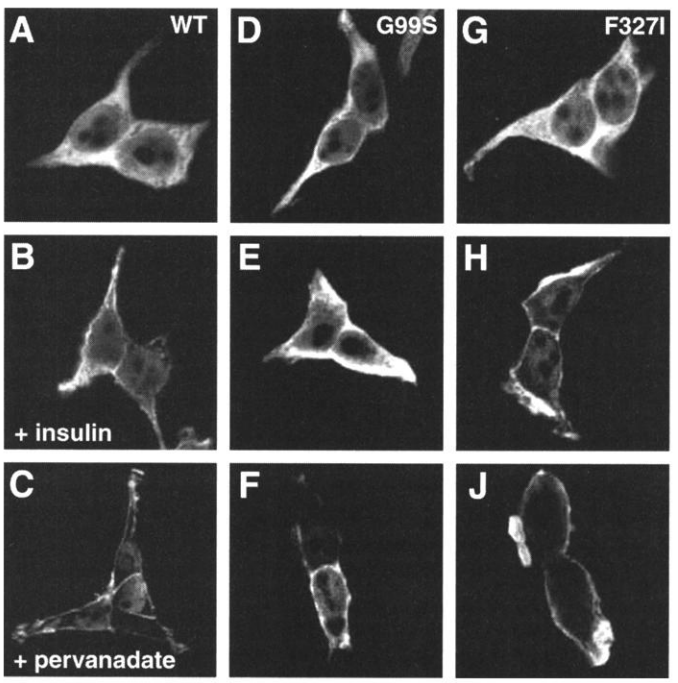

Fig. 2. Reduced membrane localization of the G99S mutation of dAkt. HEK 293 cells plated on coverslips were transfected with epitope-tagged wild-type (**A** to **C**), G99S (**D** to **F**), and F327I (**G** to **J**) dAkt and deprived of serum for 16 hours before stimulation with insulin (B, E, H) or pervanadate (C, F, J) for 5 min. Fixed and permeabilized cells were incubated first with the monoclonal antibody 12CA5 to the HA epitope and then with fluorescein isothiocyanate–conjugated secondary antibody. An analysis by confocal microscopy revealed the subcellular localization of the dAkt variants.

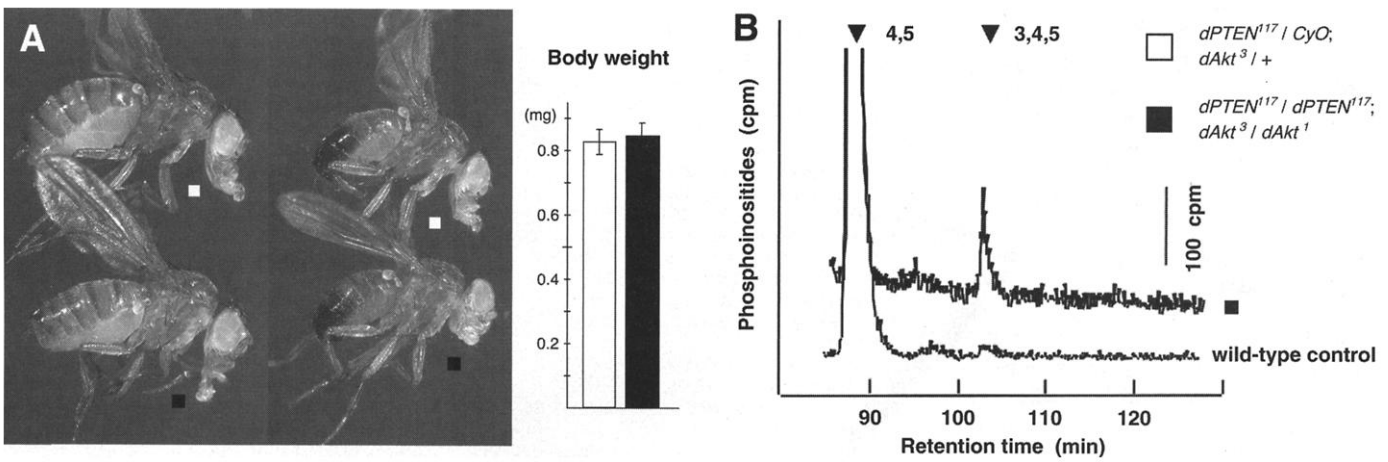

Fig. 3. Restored viability of flies lacking dPTEN function by the PH domain mutation in dAkt. (**A**) Morphology and weight of *dPTEN* mutant flies rescued by $dAkt^{3}/dAkt^{1}$. The left panel shows female flies, the middle panel shows male flies, and the right panel shows the weight of adult male flies. (**B**) PIP3 concentrations in flies devoid of dPTEN function rescued by the $dAkt^{3}$ mutation.

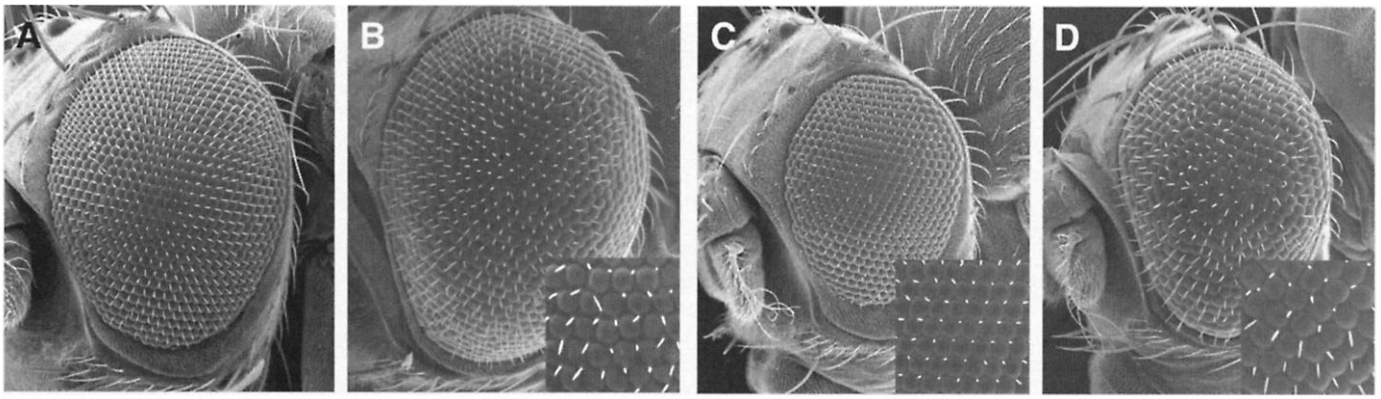

Fig. 4. Growth in the developing *Drosophila* eye promoted by activated dAkt. (**A** to **D**) Scanning electron micrographs of compound eyes of female flies; the anterior is to the left. (A) Wild type. (B) Overexpressing a membrane-tethered version of dAkt (*GMR-Gal4 UAS-myr-dAkt*). (C) *chico* mutant. (D) *GMR-Gal4 UAS-myr-dAkt* in a *chico* mutant background (*45*).

Consistently, pervanadate treatment stimulated dAktG99S activity to 80% of the wild-type level. However, pervanadate-induced activation of the mutant protein occurred more slowly than did that of the wild-type kinase (*30*). Taken together, these data indicate that the G99S substitution reduces the association of dAkt with the plasma membrane, probably by affecting the affinity of its PH domain for PIP3. Thus, $dAkt^{3}$ enabled us to study the consequences of impaired recruitment of dAkt to the plasma membrane.

We combined the *dAkt* alleles with null mutations in *dPTEN* (*32*). Animals lacking dPTEN function die during larval stages. A reduction in *dAkt* expression using the viable $dAkt^{4226}$ allele did not rescue the lethality associated with *dPTEN*. Similarly, animals doubly mutant for *dPTEN* and $dAkt^{1}$ did not survive. Thus, either dAkt activation is not the sole reason for the lethality caused by loss of PTEN, or dAkt function is not dispensable in the absence of dPTEN. The latter hypothesis is strongly supported by results obtained with the *dAkt* allele that selectively impairs the membrane recruitment of dAkt. Flies devoid of functional dPTEN were rescued to viability by any *dAkt* allelic combination that included $dAkt^{3}$ (Fig. 3A) (*33*). The rescued flies did not display morphological defects that would be expected in light of the phenotypes ascribed to clones of *dPTEN* mutant cells (*17*). Tangential sections through compound eyes revealed essentially normal ommatidial and rhabdomeric structures, and the wings of the rescued flies showed no abnormalities in the venation, such as missing crossveins (*34*). We determined the PIP3/PIP2 ratio by metabolic labeling of phospholipids from larvae (*35*). PIP3 concentrations were increased in the *dPTEN dAkt* doubly mutant larvae as compared to those of wild-type larvae (Fig. 3B), excluding the possibility that PIP3 concentrations remain within physiological limits by a feedback regulation mechanism involving dAkt. This suggests that the potential activation of a number of PH domain–containing proteins other than dAkt does not interfere with viability.

Our results indicate that the activation of dAkt is the only crucial outcome of the loss of dPTEN function. Activation of dAkt should therefore mimic the dPTEN loss-of-function phenotype. We expressed a constitutively activated membrane-anchored dAkt during eye development (*36*). The resulting eyes were increased in size due to enlarged ommatidia (Fig. 4B), a phenotype similar to that seen in clones of *dPTEN* mutant cells (*17–19*). This overgrowth phenotype is independent of upstream signals, because it was still evident in a *chico* or *Dp110/PI3K* mutant background (Fig. 4D) (*34*).

We conclude that flies devoid of the tumor suppressor dPTEN can live with abnormally high concentrations of PIP3 if only the affinity of dAkt for PIP3 is decreased. Thus, the PH domain–mediated translocation of dAkt to the membrane and its subsequent activation is the only lethal event triggered by increased PIP3 concentrations. Because the PH domain of Akt interacts with the substrate of PTEN's lipid phosphatase activity, we also conclude that PTEN does not exert any essential function other than the dephosphorylation of PIP3.

References and Notes

1. L. Simpson, R. Parsons, *Exp. Cell Res.* **264**, 29 (2001).
2. J. Li *et al.*, *Science* **275**, 1943 (1997).
3. P. A. Steck *et al.*, *Nature Genet.* **15**, 356 (1997).
4. D. M. Li, H. Sun, *Cancer Res.* **57**, 2124 (1997).
5. M. Tamura *et al.*, *Science* **280**, 1614 (1998).
6. J. Gu *et al.*, *J. Cell Biol.* **146**, 389 (1999).
7. T. Maehama, J. E. Dixon, *J. Biol. Chem.* **273**, 13375 (1998).
8. ———, *Trends Cell Biol.* **9**, 125 (1999).
9. V. Stambolic *et al.*, *Cell* **95**, 29 (1998).
10. H. Sun *et al.*, *Proc. Natl. Acad. Sci. U.S.A.* **96**, 6199 (1999).
11. B. Vanhaesebroeck *et al.*, *Annu. Rev. Biochem.* **70**, 535 (2001).
12. S. J. Leevers, B. Vanhaesebroeck, M. D. Waterfield, *Curr. Opin. Cell Biol.* **11**, 219 (1999).
13. S. Ogg, G. Ruvkun, *Mol. Cell* **2**, 887 (1998).
14. E. B. Gil, E. Malone Link, L. X. Liu, C. D. Johnson, J. A. Lees, *Proc. Natl. Acad. Sci. U.S.A.* **96**, 2925 (1999).
15. V. T. Mihaylova, C. Z. Borland, L. Manjarrez, M. J. Stern, H. Sun, *Proc. Natl. Acad. Sci. U.S.A.* **96**, 7427 (1999).
16. J. P. Rouault *et al.*, *Curr. Biol.* **9**, 329 (1999).
17. D. C. I. Goberdhan, N. Paricio, E. C. Goodman, M. Mlodzik, C. Wilson, *Genes Dev.* **13**, 3244 (1999).
18. H. Huang *et al.*, *Development* **126**, 5365 (1999).
19. X. Gao, T. P. Neufeld, D. Pan, *Dev. Biol.* **221**, 404 (2000).
20. M. A. Lawlor, D. R. Alessi, *J. Cell Sci.* **114**, 2903 (2001).
21. J. Downward, *Curr. Opin. Cell Biol.* **10**, 262 (1998).
22. P. J. Coffer, J. Jin, J. R. Woodgett, *Biochem. J.* **335**, 1 (1998).
23. T. O. Chan, S. E. Rittenhouse, P. N. Tsichlis, *Annu. Rev. Biochem.* **68**, 965 (1999).
24. S. Paradis, G. Ruvkun, *Genes Dev.* **12**, 2488 (1998).
25. B. E. Staveley *et al.*, *Curr. Biol.* **8**, 599 (1998).
26. J. Verdu, M. A. Buratovich, E. L. Wilder, M. J. Birnbaum, *Nature Cell Biol.* **1**, 500 (1999).
27. S. E. Scanga *et al.*, *Oncogene* **19**, 3971 (2000).
28. A. C. Spradling *et al.*, *Genetics* **153**, 135 (1999).
29. The $dAkt^{3}$ allele was found in a collection of homozygous viable mutations from Ch. Zuker and E. Koundakjian (University of California, San Diego) because it yields flies of severely reduced body size.
30. M. Andjelkovic, B. A. Hemmings, unpublished results.
31. M. Andjelkovic *et al.*, *Proc. Natl. Acad. Sci. U.S.A.* **93**, 5699 (1996).
32. The *dPTEN* alleles used are $dPTEN^{dJ189}$ (*19*) and $dPTEN^{117}$ (*37*). Both are presumably null alleles. We also tested them over a deficiency lacking the *dPTEN* locus, *Df(2L)170B*. Because this deficiency also lacks *chico*, an upstream component of insulin receptor signaling, we reintroduced *chico* by means of a genomic rescue construct. In all cases, we obtained similar results.
33. Whereas the strongest allelic combination $dAkt^{1}/dAkt^{3}$ completely rescued the *dPTEN* mutant flies to wild-type size, the combinations $dAkt^{3}/dAkt^{3}$ and $dAkt^{3}/dAkt^{4226}$ could rescue the lethality associated with loss of PTEN function, but the resulting flies were slightly enlarged. Furthermore, we observed a variability of the phenotypes in all combinations. Consistently, flies that emerged earlier showed a tendency to be of increased size, whereas some retarded flies were of smaller size.
34. H. Stocker, E. Hafen, unpublished results.
35. Nonwandering third instar larvae were phosphate starved in phosphate-free Schneider S2 medium and then labeled with 2 mCi per sample of inorganic ^{32}P (50 mCi/ml). PIP3 and PIP2 levels were determined according to (*38*).
36. To anchor dAkt to the plasma membrane, the myristoylation-palmitoylation motif from the Lck tyrosine kinase was fused to the NH_2-terminus of hemagglutinin (HA) epitope–tagged dAkt, as previously described for mammalian Akt (*39*). Analysis of the subcellular localization by immunofluorescence using the epitope antibody to HA confirmed the constitutive membrane localization of myr-dAkt.

37. S. Oldham, E. Hafen, unpublished results.
38. A. Arcaro, M. P. Wymann, *Biochem. J.* **296**, 297 (1993).
M. Andjelkovic *et al.*, *J. Biol. Chem.* **272**, 31515 (1997).
40. M. Andjelkovic *et al.*, *J. Biol. Chem.* **270**, 4066 (1995).
41. Single-letter abbreviations for the amino acid residues are as follows: A, Ala; E, Glu; F, phe; G, Gly; I, Ile; P, Pro; R, Arg; S, Ser; and T, Thr.
42. dAkt was immunoprecipitated from wild-type and *dAkt*^{3} larvae with a rabbit polyclonal antibody raised against recombinant dAkt-66 (*40*). In vitro kinase assays were performed, as described, using the peptide GRPRTSSAEG (*41*) as a substrate (*39*).
43. HEK 293 cells were transfected by a modified calcium phosphate method, as described (*39*). The transfection mixture was removed after a 16-hour incubation, and cells were serum-starved for 24 hours before stimulation with 0.5 to 1 μM insulin (Boehringer Mannheim).
44. The HA epitope–tagged dAkt proteins were immunoprecipitated from 100 μg of cell-free extracts using the monoclonal antibody 12CA5 coupled to protein A–Sepharose. In vitro kinase assays were performed, as described (*39*).
45. The size difference of the eyes in Fig. 4, B and D, is entirely due to varying numbers of ommatidia. The size of the ommatidia, however, is comparable (insets) and massively larger than in *chico* mutants (inset in 4C). The failure of myr-dAkt to compensate for the reduced number of ommatidia in *chico* mutants is consistent with the late onset of expression driven by *GMR-Gal4*.
46. We thank Ch. Zuker and E. Koundakjian for the *dAkt*^{3} allele; T. Radimerski for the S2 labeling medium; T. Gutjahr, Ch. Hugentobler, R. Bopp, P. Zipperlen, P. Cron, P. Müller, and H. Angliker for technical support; K. Basler and P. Gallant for critical reading of the manuscript and valuable suggestions; and D. Pan and S. Leevers for providing fly stocks. Supported by grants from the Schweizerische Krebsliga (B.A.H. and M.P.W.) and the Swiss National Science Foundation (E.H.).

15 November 2001; accepted 12 February 2002

Reverse Transcriptase–Mediated Tropism Switching in *Bordetella* Bacteriophage

Minghsun Liu,[1] Rajendar Deora,[1]* Sergei R. Doulatov,[1]* Mari Gingery,[1] Frederick A. Eiserling,[1] Andrew Preston,[2] Duncan J. Maskell,[2] Robert W. Simons,[1] Peggy A. Cotter,[3] Julian Parkhill,[4] Jeff F. Miller[1]†

Host-pathogen interactions are often driven by mechanisms that promote genetic variability. We have identified a group of temperate bacteriophages that generate diversity in a gene, designated *mtd* (major tropism determinant), which specifies tropism for receptor molecules on host *Bordetella* species. Tropism switching is the result of a template-dependent, reverse transcriptase–mediated process that introduces nucleotide substitutions at defined locations within *mtd*. This cassette-based mechanism is capable of providing a vast repertoire of potential ligand-receptor interactions.

The infectious cycles of *Bordetella* subspecies, which cause respiratory infections in humans and other mammals, is controlled by the BvgAS signal transduction system (*1*). Using a multistep phosphorelay, the BvgS transmembrane sensor-kinase and the BvgA transcriptional regulator couple environmental signals to expression of cell surface and secreted molecules (*1*, *2*). The Bvg$^+$ phase, which is necessary and sufficient for respiratory tract colonization, is characterized by a high level of BvgAS activity and expression of virulence and colonization factors that include adhesins, toxins, and a type III secretion system (*2*). In the Bvg$^-$ phase, BvgAS is inactive, virulence and colonization factors are not expressed, and numerous genes are induced, including motility loci in *Bordetella bronchiseptica* and virulence repressed genes in *Bordetella pertussis* (*2*, *3*). The Bvg$^-$ phase appears to be adapted to ex vivo growth and survival in *B. bronchiseptica* (*4*). Recent evidence suggests that BvgAS is capable of controlling a spectrum of distinct phenotypic phases in response to subtle changes in signal intensity (*5*, *6*).

In a search for generalized transducing vectors, we identified several temperate bacteriophages present in clinical isolates of *B. bronchiseptica* that displayed a marked tropism for Bvg$^+$ as opposed to Bvg$^-$ phase bacteria. The efficiency of plaque formation of a representative phage, designated BPP-1 (Bvg plus tropic phage–1), was 10^6-fold higher on Bvg$^+$ phase RB50 (wild-type *B. bronchiseptica*) than on an isogenic Bvg$^-$ phase-locked strain (Δ*bvgS*) (Fig. 1A). An adsorption assay (Fig. 1B) indicated that the BPP-1 receptor is specifically expressed in the Bvg$^+$ phase. Mutagenesis of loci encoding Bvg$^+$ phase surface factors showed that deletion of *prn*, which encodes the adhesin pertactin (*7*), eliminated BPP-1 adsorption and decreased phage plaquing to a level similar to that observed on Bvg$^-$ phase cells (Fig. 1, A and B). Ectopic expression of *prn*

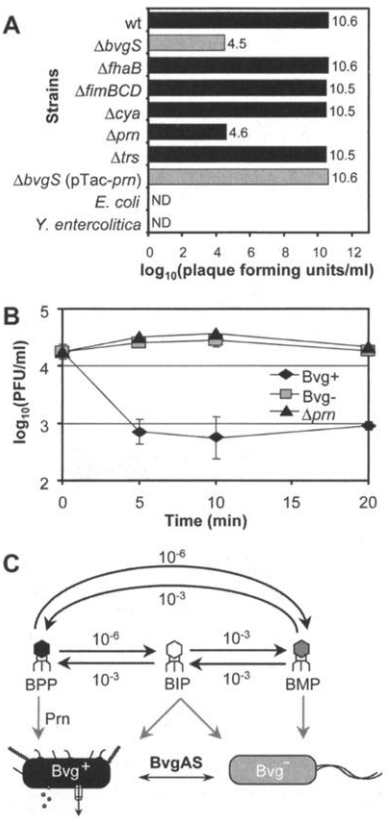

Fig. 1. (**A**) Efficiency of plaquing by a high-titer BPP-1 lysate [4×10^{10} plaque forming units/ml (pfu/ml)] on isogenic *B. bronchiseptica* mutants. The Δ*bvgS*, Δ*fhaB*, Δ*fimBCD*, Δ*cyaA*, Δ*prn*, and Δ*trs* mutations are in-frame deletion mutations that eliminate BvgS activity or expression of FHA (filamentous hemagglutinin), fimbriae, adenylate cyclase toxin, pertactin, or the type III secretion apparatus. Black bars indicate Bvg$^+$ phase strains; gray bars indicate strains genetically locked in the Bvg$^-$ phase. pTac-prn is a complementing plasmid that expresses pertactin under control of the Tac promoter. *E. coli* strain DH5α and *Yersinia enterocolitica* strain JB580v did not support phage growth. ND, no plaque detected. (**B**) BPP-1 adsorption assay (*8*) with the use of wild-type *B. bronchiseptica* strain RB50 (*4*), isogenic Bvg$^-$ (Δ*bvgS*), and Δ*prn* derivatives, all grown under Bvg$^+$ phase conditions. (**C**) Summary of tropism switching frequencies by *Bordetella* phages. A spontaneous mutant resistant to BIP-1 but still sensitive to BPP-1 and BMP-1 were used to obtain switching frequencies from BIP-1 to BPP or BMP tropic variants.

[1]Department of Microbiology, Immunology and Molecular Genetics, University of California, Los Angeles, Los Angeles, CA 90095, USA. [2]Centre for Veterinary Science, Department of Clinical Veterinary Medicine, University of Cambridge, Cambridge CB3 OES, UK. [3]Department of Molecular, Cellular and Developmental Biology, University of California, Santa Barbara, Santa Barbara, CA 93106, USA. [4]The Sanger Centre, The Wellcome Trust Genome Campus, Hixton, Cambridge, UK.

*These authors contributed equally to this work.
†To whom correspondence should be addressed. E-mail: jfmiller@ucla.edu.